Available online at www.sciencedirect.com
SCIENCE DIRECT®
ELSEVIER
Journal of Magnetism and Magnetic Materials 286 (2005) 356–361
Journal of magnetism and magnetic materials
www.elsevier.com/locate/jmmm

Dynamic and static magnetic anisotropy in thin-film cobalt zirconium tantalum

J.P. Nibarger[a,*], R.L. Ewasko[a], M.L. Schneider[b], T.J. Silva[b]

[a]*Storage Technology Corp., One StorageTek Drive, Louisville, CO 80028-4274, USA*
[b]*National Institute of Standards and Technology, Electromagnetics Division, Boulder, CO 80305, USA*

Available online 26 October 2004

Abstract

The magnetic anisotropy values of thin amorphous cobalt zirconium tantalum (CZT) films were determined from static and dynamic measurements. Dynamic techniques show a rotatable component of anisotropy that decreases with increasing longitudinal bias field from 200 to 0 ± 48 A/m (2.5 to 0 ± 0.6 Oe). The dynamic value of the anisotropy is important when using CZT in high-frequency magnetic applications. Static values were obtained with an induction-field magnetometer while dynamic values were obtained using a pulsed inductive microwave magnetometer.

PACS: 75.30.Gw; 75.40.Gb; 75.70.Ak; 75.50.Kj

Keywords: Anisotropy; CZT; Magneto-dynamics; PIMM; Rotatable anisotropy

As the magnetic recording industry increases data transfer rates, the characterization of magnetic materials must also be performed at higher frequencies. The pulsed inductive microwave magnetometer (PIMM) is ideally suited to help with such characterization because it measures the damped gyromagnetic response in the time domain [1].

The PIMM can be used to identify the symmetry of the dynamic anisotropy which can differ from the static anisotropy [2]. In order to utilize these techniques, we must vary the angle between the easy-axis and a static applied magnetic bias field. Misalignment between the direction of the magnetization and the applied static magnetic bias field must be taken into account when analyzing such data. Sources of this misalignment can arise in the films from an in-plane magnetic anisotropy field or an out-of-plane demagnetization field. This misalignment is often referred to as "dragging", and has been seen in ferromagnetic resonance (FMR) experiments [3,4]. In this report, we use angle-resolved PIMM data, corrected for the dragging effect, to determine the dynamic anisotropy of cobalt zirconium tantalum (CZT).

*Corresponding author. Tel.: +303 661 2837; fax: +303 661 8992.
E-mail address: john_nibarger@storagetek.com (J.P. Nibarger).

0304-8853/$ - see front matter © 2004 Elsevier B.V. All rights reserved.
doi:10.1016/j.jmmm.2004.09.077

A Co-rich (92% Co) CZT sample was prepared using DC magnetron sputtering with a magnetic field applied during deposition. The 131 nm thick CZT was deposited on a thermally oxidized (1 0 0) oriented silicon substrate. The magnetostriction of this sample was negligible (2.6×10^{-7}) [5], as measured with an optically based cantilever method [6].

Static measurements were performed using a 50 Hz induction-field (*B-H*) magnetometer [7]. The inset in Fig. 1 shows the easy and hard-axis hysteresis loops. The static anisotropy, H_k^{stat} was determined by measuring the hard-axis hysteresis loops as a function of an applied transverse bias field H_b^T applied along the easy-axis. Fig. 1 shows the measured values of M_s/χ_0 as a function of H_b^T. Fitting the data to the equation $M_s/\chi_0 = H_k^{\text{stat}} + H_b^T$ yields an asymptotic value for H_k^{stat}. The determined value of H_k^{stat} is 1597 ± 4.6 A/m (20.07 ± 0.06 Oe), where the error bars on the data points represent a 2σ value.

The dynamic measurements were performed using a PIMM with 220, 525, and 990 μm wide center-conductor coplanar waveguides (CPW). The easy-axis of the CZT film was oriented at different angles with respect to the center conductor of the CPW using a rotation stage. A commercial pulse generator provided pulses with a 50 ps rise time and 10 ns duration. Using the Karlqvist equation [8] for fields produced by a current strip we calculated that our 3.16 V pulse yielded a field of 88.6 A/m (1.11 Oe).

Orthogonal Helmholtz coil pairs were used to produce the bias fields and saturation fields used in the measurements. The field at the sample had a 1% variation across its area. The precessional response was measured with a 20 GHz digital sampling oscilloscope. A longitudinal bias field H_b, was applied parallel to the center conductor as shown in Fig. 2, while the saturation field was applied parallel to the pulse field. The resonance frequency ranged from 2.9 to 4.2 GHz, well within the measurable bandwidth of the system.

The magnetic precessional response of the CZT film was measured in the time domain then converted into the frequency domain using a fast Fourier transform. The resonance frequency was determined by the zero crossing of the real part of the susceptibility [9]. The Kittel formula [10] was used to determine the anisotropy of the sample. The slope of ω^2 versus H_b along the easy-axis yielded a value for the Landé g-factor of 2.175. Such a large value for g is consistent with previous results for Co-rich systems [7]. The x-intercept provided the dynamic anisotropy, H_k^{dyn}, using a measured saturation magnetization value of

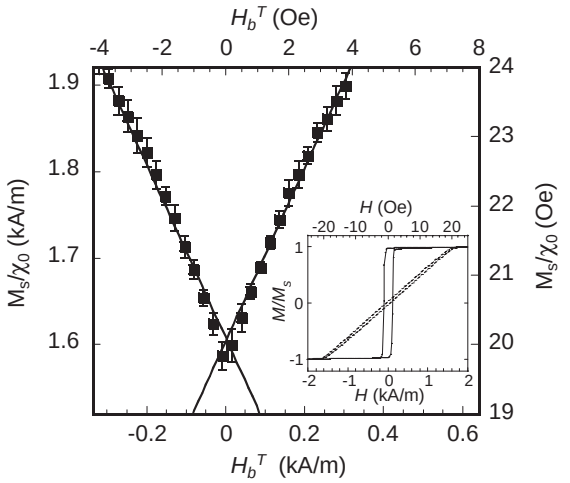

Fig 1. Static inductive looper data for reciprocal normalized susceptibility M_s/χ_0 versus transverse bias field H_b^T oriented along the easy-axis direction. By determining the susceptibility as a function of transverse bias field, the static anisotropy is extracted as the asymptotic value when $H_b^T = 0$. Error bars represent 2σ statistical error. Inset shows the measured easy and hard-axis hysteresis loops without transverse bias field.

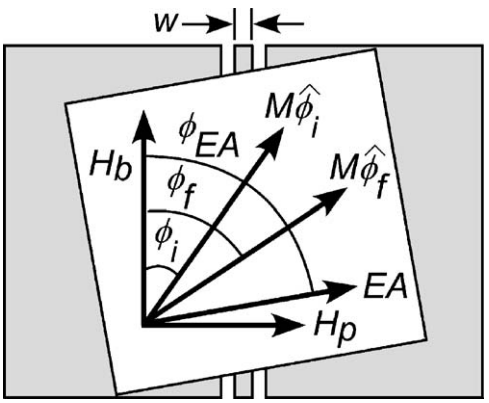

Fig 2. Experimental geometry of the angle-resolved PIMM meansurements.

$\mu_0 M_s = 1.4\,\mathrm{T}$. The saturation magnetization $\mu_0 M_s$ was measured on 150 mm-diameter wafers using a calibrated *B-H* looper.

Dynamic measurements of the anisotropy were made at varying angles of ϕ_{EA} (see Fig. 2), from 0 to 360° in increments of 3.6°, as shown in Fig. 3. The data have been corrected for the effect of the finite width of the waveguide [11]. The correction arises from internal dipolar fields that can be represented as

$$H_k^{MSSW} = \frac{\pi}{4} M_S \frac{\delta}{w}, \tag{1}$$

where H_k^{MSSW} is an additional stiffness field used in the Kittel equation, w is the CPW center conductor width and δ is the thickness of the sample. This correction was calculated using the thin film limit and experimentally verified [11]. In addition, we have experimentally verified the validity of Eq. (1) by performing measurements with three different center conductor widths (220, 525, and 990 μm).

Fig. 2 presents a schematic of the sample magnetization. If the applied bias field H_b is zero, the magnetization **M** points along the easy-axis at an angle ϕ_{EA} with respect to the CPW center conductor, $\mathbf{M} = M\hat{\phi}_{EA}$. With the addition of an applied bias field H_b, $\mathbf{M} = M\hat{\phi}_i$ lies between the easy-axis and H_b at an angle ϕ_i. With the application of a field pulse H_p, **M** moves further away from H_b to an angle ϕ_f between the easy-axis and H_b. In essence, the angle of the sample set by the experimenter (ϕ_{EA}) is not the same as the angle of the magnetization (ϕ_f) when the pulse is applied. Therefore, an angle-resolved plot of magnetic anisotropy reflects the angle of the sample and not the angle of the magnetization. We present below a method to account for the dragging effect in our experimental geometry. For easy-axis measurements, both ϕ_i and ϕ_{EA} are equal to zero, so no dragging effect exists.

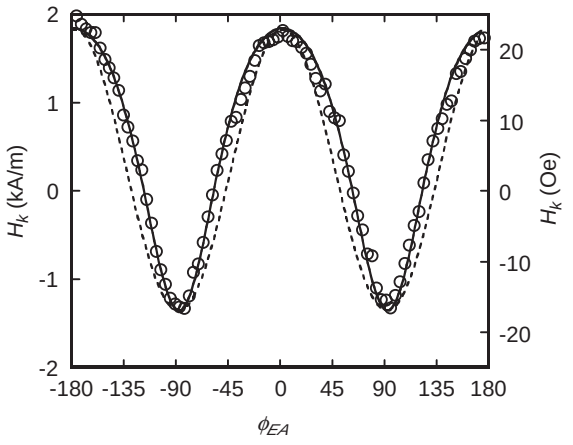

Fig 3. Experimental results of angle-resolved PIMM measurements are shown in open circles where 2σ error bars on the measurement are smaller than the data points. The solid line represents the simulated results including dragging effects, using a fitted value for $H_k^{(0)}$. The dashed line represents a comparison of the data to Eq. (8) with no dragging, i.e. in the limit of $H_b \gg H_k^{(2)}$.

We can analytically model the dragging effect, starting with the Zeeman energy of the system that is given by

$$U_Z(H_b, H_p, \phi) = -\mu_0 M_s H_b \cos(\phi) - \mu_0 M_s H_p \sin(\phi), \tag{2}$$

where μ_0 is the permeability of free space, M_s is the saturation magnetization, H_b is the applied bias field, H_p is the pulse field, ϕ is the angle between H_b and the magnetization. We also account for the anisotropy energy as follows:

$$U_k(\phi, \phi_i, \phi_{EA}) = -\frac{\mu_0}{2} M_s (H_k^{(0)} \cos^2(\phi - \phi_i) + H_k^{(2)} \cos^2(\phi - \phi_{EA})), \tag{3}$$

where $H_k^{(0)}$ and $H_k^{(2)}$ are the rotatable and uniaxial anisotropy fields, respectively, and ϕ_i is the angle between the magnetization and H_b when $H_p = 0$. In order to determine the final equilibrium angle ϕ_f, we minimize the energy of the magnetization when the field pulse is on:

$$\frac{d}{d\phi}(U_Z(H_b, H_P, \phi) + U_k(\phi, \phi_i, \phi_{EA}))\Big|_{\phi_f} = 0. \tag{4}$$

The second derivative of the energy with respect to ϕ is the stiffness field $\tilde{H}$. The stiffness field was used in the Kittel equation [10] to calculate the ferromagnetic precession frequency given by

$$\tilde{H}(H_b, H_p, \phi_f, \phi_i) = \frac{1}{\mu_0 M_S} \frac{d^2}{d\phi^2}(U_Z(H_b, H_p, \phi) + U_k(\phi, \phi_i))\Big|_{\phi_f}. \tag{5}$$

In the limit where $M_s \gg H_{total}$, the Kittel equation is well approximated by

$$\omega(H_b, H_p, \phi_f, \phi_i) \approx |\gamma|\mu_0\sqrt{M_s\tilde{H}(H_b, H_p, \phi_f, \phi_i)}. \quad (6)$$

The stiffness field, from Eq. (5), is given by

$$\tilde{H}(H_b, H_p, \phi_f, \phi_i) = H_b\cos(\phi_f) + H_p\sin(\phi_f) + H_k^{dyn}(\phi_f, \phi_i). \quad (7)$$

where

$$H_k^{dyn}(\phi_f, \phi_i) = H_k^{(0)}\cos(2(\phi_f - \phi_i)) + H_k^{(2)}\cos(2\phi_f). \quad (8)$$

Dynamic measurements of the precession frequency were performed with varying angle ϕ_{EA}. The bias field H_b was varied from 1.6 to 8.8 kA/m (20 to 110 Oe) in 160 A/m (2 Oe) steps. Using the Kittel equation [9], we determined the dynamic anisotropy H_k^{dyn} as the negative value of the x-intercept in a plot of ω^2 versus H_b for a range of values of H_b. The range of values for H_b spanned 4 kA/m (50 Oe) and had varying initial fields from 1.6 to 4.8 kA/m (20–60 Oe) in steps of 0.4 kA/m (5 Oe). An example of an angle-resolved scan with a field span of 4.8–8.8 kA/m (60–110 Oe) is shown in Fig. 3 with open circles.

We propose a way to account for the dragging effect in analysis of angle-resolved PIMM data. First, for bias fields and angles matching our experimental conditions, we calculated ϕ_f for a given set of fields and ϕ_{EA} angles. We used this information in the above analytical dragging model to simulate data under our experimental conditions and obtained a plot of the anisotropy versus ϕ_{EA}. We also simulated the data with no dragging effect to extract the influence of the dragging effect on a plot of $H_{k,eff}$ versus ϕ_{EA}. Applying this tequnique, we use the value of $H_k^{(2)}$ as determined by static hysteresis measurements. To determine $H_k^{(0)}$, Fourier transforms of both the experimental data and the simulated curves were generated. The theoretical seed value for $H_k^{(0)}$ was iteratively varied until there was no difference in the DC Fourier components between the experimental and simulated results. The simulation results are shown as the solid line in Fig. 3. The simulated curve in Fig. 3 has only two adjustable parameters: $H_k^{(0)}$ and a uniform correction to the applied bias field angle. All other parameters are fixed. The data are also corrected for dipolar effects (Eq. (1)) due to the finite center conductor width [11]. In the absence of dragging, one would expect the data to follow the functional form of $H_{k,eff}(\phi_f)$ with respect to ϕ_{EA}. Fig. 3 shows a dashed line with this functional form to demonstrate the necessity of accounting for the dragging effect. In addition, as mentioned above, the field range over which the data are analyzed has an effect on the determined value of anisotropy. A plot of the value of $H_k^{(0)}$ as a function of the analyzed field range is shown in Fig. 4 as open squares.

It is also possible to extract a value for the uniaxial anisotropy component from the angle-resolved PIMM data, independent of the statically measured value. To accomplish this, we perform a Fourier transform on the simulated curve as a function of ϕ_{EA} to extract an effective anisotropy spectrum:

$$H_{k,sim}(\phi_{EA}) = \sum_{n=0} H_{k,sim}^{(2n)}\cos(2n\phi_{EA}). \quad (9)$$

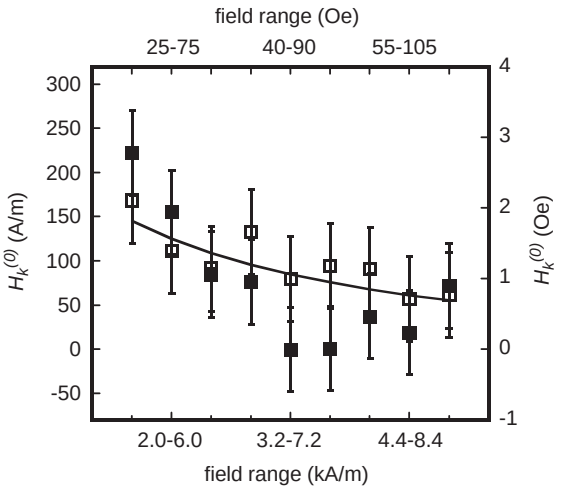

Fig. 4. Experimental results for the difference between the measured dynamic anisotropy and the static anisotropy. Solid squares are for data taken using the easy-axis method and open squares are for data taken using the rotational method. The curve is a fit to the data using Eq. (13) where the field used was the average field of the range plus H_k which gave a value of δ to be $2^\circ \pm 0.2^\circ$.

We find that the dragging effect has a small influence on the uniaxial component of the simulated data. The simulation used an initial seed value for the uniaxial anisotropy of $H_k^{(2)} = 1597\,\mathrm{A/m}$ (20.07 Oe). This initial condition yielded a result for $H_{k,\mathrm{sim}}^{(2n)}$ of 1555 A/m (19.54 Oe). The difference between the seed value and the value extracted from the simulation is then corrected in the actual data. The extracted uniaxial anisotropy from a Fourier transform of the data is 1474 A/m (18.52 Oe). Adding the dragging correction, we determine the dynamic uniaxial component to be $H_k^{(2)} = 1530 \pm 10.4\,\mathrm{A/m}$ (19.22 ± 0.13 Oe), which is 5% less than the statically determined value of 1600 A/m (20.07 Oe). We find that the 4th- and higher-order harmonics are within the noise of the data. The noise in the data is estimated by determining the average value of the Fourier amplitudes, using only the 10th harmonic and higher, with a resultant value of 5.6 A/m (0.07 Oe). Using this criterion the 4th and higher harmonic components in the experimental anisotropy spectrum based upon Eq. (9) are comparable to the spectral noise.

In order to confirm our correction technique a second method of dynamically measuring the anisotropy was employed. This method involves measurements made when the easy-axis is aligned with the bias field. In this configuration, there is no dragging effect. In this method, H_k^{dyn} is determined from the Kittel equation [9] as a function of the bias field range. The rotatable anisotropy component $H_k^{(0)}$ is found by taking the difference between the dynamic and static uniaxial components ($H_k^{(0)} = H_k^{\mathrm{dyn}} - H_k^{\mathrm{stat}}$) and is plotted as solid squares in Fig. 4.

In both techniques, we find that there is an upturn in the measured value of $H_k^{(0)}$ when the data are analyzed at lower bias fields. We believe that this is a phenomenon not related to dragging. When we are measuring on the easy-axis we are aligned to better than 0.4°. At this level of alignment the dragging effect on the easy-axis data is too small to account for the upturn. We speculate that the upturn in the value of $H_k^{(0)}$ with decreasing field may be due to variations in the direction of the anisotropy field in the material.

The magnetic energy of the system can be written with this new angular deviation δ as

$$U = -\mu_0 M_s \left(\frac{H_k}{2} \cos^2(\theta + \delta) + H_b \cos\theta \right), \qquad (10)$$

where the angle θ corresponds to the angle between the magnetization and the easy-axis.

The average angle $\langle\theta\rangle$ can be found by minimizing the energy with respect the angle θ and solving

$$\langle\theta\rangle = -\frac{H_k \delta}{H + H_k}. \qquad (11)$$

The self-energy of the system with an average angle $\langle\theta\rangle$ at an angle of Ω is given by

$$U_{k,r} = -\frac{\mu_0}{2} M_s^2 \sin^2\langle\theta\rangle \sin^2\Omega. \qquad (12)$$

$M_s \sin^2\langle\theta\rangle$ in Eq. (12) scales as an anisotropy energy term, which we write as $H_k^{(0)} = M_s \sin^2\langle\theta\rangle$. Substituting the value for $\langle\theta\rangle$ from Eq. (11) we arrive at the following relationship between the dispersion angle δ and the rotatable anisotropy:

$$H_k^0 = M_s \left(\frac{H_k \delta}{H + H_k} \right)^2. \qquad (13)$$

The data in Fig. 4 has been fit to Eq. (13) with only δ as an adjustable parameter. The fit yielded a value of $2.1^\circ \pm 0.2^\circ$. A measure of this dispersion has been performed using a calibrated *B-H* looper and yields an angular deviation of 0.83°. We see that an upturn in the data at low bias fields is expected from this simple model. And we note reasonable agreement between the measured angular deviation and our crude model.

In conclusion, we have used the angle-resolved PIMM technique to measure the magnetic anisotropy of CZT thin films with an estimated error of 48 A/m (0.6 Oe). We find that measurements with a PIMM must take into account the misalignment of $\boldsymbol{M}$ with respect to the applied bias field. We are able to accurately model this dragging effect to quantitatively estimate the errors induced for angle-resolved data. In order to avoid nonlinear fitting errors, we evaluate Fourier transforms for the data and simulated results. By comparing the simulated and measured spectral components, we can correct for dragging. We verified the validity

of our modeling technique by performing measurements with an easy-axis alignment. We found that there is an upturn in the $H_k^{(0)}$ term when analyzing the data at low fields. We speculate that this upturn may be due to angular dispersion in the sample.

Acknowledgment

The authors express their sincere gratitude to Zbigniew Celinski for important assistance in analyzing the data obtained in this work.

References

[1] T.J. Silva, C.S. Lee, T.M. Crawford, C.T. Rogers, J. Appl. Phys. 85 (1999) 7849.
[2] R. Lopusnik, J.P. Nibarger, T.J. Silva, Z. Celinski, Appl. Phys. Lett. 83 (2003) 96.
[3] A.F. Kip, R.D. Arnold, Phys. Rev. 75 (1949) 1556.
[4] A.H. Morrish, The Physical Principles of Magnetism, IEEE, New York, 1965.
[5] Y. Hoshi, H. Kazama, M. Naoe, S. Yamanaka, IEEE Trans. Magn. 19 (1983) 1958.
[6] A.C. Tam, H. Schroeder, IEEE Trans. Magn. 25 (1989) 2629.
[7] R.M. Bozorth, Ferromagnetism, Wiley, New York, 1993.
[8] O. Karlquist, Trans. R. Inst. Tech. Stockholm 86 (1954) 3.
[9] N.X. Sun, S.X. Wang, T.J. Silva, A.B. Kos, IEEE Trans. Magn. 38 (2002) 146.
[10] C. Kittel, Introduction to Solid State Physics, fifth ed, Wiley, New York, 1995.
[11] M.L. Schneider, A.B. Kos, T.J. Silva, Appl. Phys. Lett. 85 (2004) 032427.